International Society for Rock Mechanics and Rock Engineering
Norwegian Group for Rock Mechanics

ISRM International Symposium
Eurock 2025 – Expanding the Underground Space
Trondheim, Norway, 16-20 June
ISBN 978-82-8208-079-8

Water-Assisted CO_2 Fracturing of Volcanic Rocks under Geothermal Conditions: Characteristics and Effectiveness

Eko Pramudyo[a], Yuto Watanabe[a], Kazumasa Sueyoshi[a], Kiyotoshi Sakaguchi[a], Jiajie Wang[a], Sho Ogata[b,c], Kazumi Osato[d], Amane Terai[e], Noriaki Watanabe[a]

[a]Department of Environmental Studies for Advanced Society, Graduate School of Environmental Studies, Tohoku University, Sendai 9808579, Japan
[b]Division of Global Architecture, Graduate School of Engineering, Osaka University, Osaka 5650871, Japan
[c]Center for Future Innovation, Graduate School of Engineering, Osaka University, Osaka 5650871, Japan
[d]Geothermal Energy Research and Development Co. Ltd. (GERD), Tokyo 1040033, Japan
[e]Japan Organization for Metals and Energy Security (JOGMEC), Tokyo 1050001, Japan
Correspondence: eko.pramudyo.c3@tohoku.ac.jp (E. Pramudyo)

Abstract

Creating geothermal reservoirs via fracturing in low permeability volcanic rocks at presently drillable depths is claimed to enhance power generation. Hereby, water-assisted CO_2 fracturing was proposed as an effective method to induce permeable fractures in volcanic rocks. In this method, water injection is used to pressurize CO_2 that initially existed in a borehole. The pressurized CO_2 will generate complex fracture pattern at low pressure, and later, the injected water will widen and propagate the induced fractures. This paper provides summary of the findings presented in Pramudyo et al. (2024, *Geoenergy Science and Engineering, 243*), which elucidated the characteristics and effectiveness of water-assisted CO_2 fracturing as a permeability enhancement method in various volcanic rock under geothermal conditions, considering the effects of pre-existing pore water and rock texture. The study involved fracturing experiments conducted at geothermal temperatures and triaxial stress conditions on water saturated samples prepared from various volcanic rocks, with the results compared to published results of fracturing on dry volcanic rock samples. Analyses revealed that pre-existing pore water inhibits fracture propagations, as shown by CO_2 fracturing experiment on water-saturated sample. Nevertheless, the inhibitory effect was diminished in water-assisted CO_2 fracturing; wider and longer fractures than those induced in CO_2 fracturing were obtained. The experiments also revealed that porosity and rock texture, such as grain size, influence the characteristics of fracture networks induced by the water-assisted CO_2 fracturing. The induced fractures are in porous volcanic rocks, such as pyroclastic rocks, than in tight rocks, such as lava. Moreover, the induced fractures tended to be wider and longer with increasing grain/clast size in pyroclastic rocks. The study suggests that water-assisted CO_2 fracturing is effective in creating complex network of wide fractures in various volcanic rock at geothermal conditions.

Keywords

Enhanced geothermal system, carbon dioxide fracturing, complex fracture network, lava, pyroclastic rocks

ISRM

NBG

1 Introduction

Developing enhanced geothermal system (EGS) reservoirs in low-permeability volcanic rocks at currently accessible drilling depths would allow for increased or optimized power generation (Yoshioka et al., 2019; Eggertsson et al., 2020). Therefore, Takuma et al. (2024) experimentally and numerically studied CO_2 and water fracturing in volcanic rocks, as permeability enhancement methods to create geothermal reservoir of c.a. 1 – 2 km deep. They showed that fractures induced by CO_2 injection had narrower apertures (thinner) compared to water induced fractures. Accordingly, this was due to smaller pressure differences between the induced fracture interior and the unfractured rock matrix, caused by effective penetration of low viscosity (< c.a. 100 μPa · s) CO_2 into the unfractured matrix, which resulted in inhibited further fracture widening and propagation. To address the narrow fracture challenge, water assisted CO_2 fracturing was proposed and demonstrated (Takuma et al., 2024). In this method, water is injected to compress CO_2 initially existed in the borehole, where complex fracture network in the rock is first created by CO_2 penetration. The injected water, having higher viscosity of > c.a. 100 μPa · s, later creates larger differential pressures, between induced fracture interior and rock matrix, that widen (increase the aperture) and propagate fractures more effectively.

Water-assisted CO_2 fracturing appears to be an effective method to obtain initial permeability enhancement. However, the method was numerically suggested and experimentally demonstrated on dry volcanic rocks (Takuma et al., 2024). Meanwhile, preexisting pore water may exist within the volcanic rock of actual geothermal environments. The preexisting pore water may affect CO_2 penetration and fracture characteristics, due to water higher viscosity as compared to that of CO_2. Therefore, it is crucial to elucidate the influence of preexisting pore water on the the characteristics of the induced fractures in water-assisted CO_2 fracturing. Additionally, it is important to clarify how variations in rock texture, such as porosity, and grain or clast sizes and their sortation, impact the fracturing characteristics. This paper summarizes the content of Pramudyo et al. (2024), which elucidated the effects of preexisting pore water and rock texture on the characteristics and effectiveness of water-assisted CO_2 fracturing in different volcanic rocks, based on new experiments and previously published experiment results in Takuma et al. (2024).

2 Material and methods

Cylindrical samples (diameter, 30 mm; length, 25 mm) with a borehole (diameter, 1.5 mm; depth, 10 mm) were prepared using Honkomatsu (lava) and Emochi (tuff) andesites from Kanagawa and Fukushima prefectures, Japan, respectively. Cylindrical samples were also prepared from dacitic and andesitic lapilli tuffs obtained from depths of c.a. 1000 and 1100 m, respectively, of a temperature survey well belonging to Japan Organization for Metals and Energy Security (JOGMEC) drilled in Hachimantai area, Iwate prefecture, Japan. Honkomatsu andesite had a massive texture (comprised of very fine grains/crystals of < c.a. 0.5 mm). Whereas Emochi andesite consisted of > c.a. 95% ash sized clasts. The dacitic lapilli tuff comprised c.a. 70% ash sized clast, and c.a. 30% lapilli sized clast with average diameter of c.a. 3mm. The andesitic lapilli tuff comprised c.a. 40 – 50% ash-sized clast, and c.a. 50 – 60 % lapilli-sized clasts with average diameter of c.a. 7 mm. Honkomatsu andesite had the lowest initial porosity (c.a. 5%) and permeability (c.a. 10^{-18} m^2), as well as the highest tensile strength (10 MPa, cohesion (40 MPa), and internal friction angle (58°). Therefore, Honkomatsu andesite is called tight rock. Whereas the pyroclastic rocks exhibit the lower tensile strength, cohesion, and internal friction angles: Emochi andesite (5 MPa, 20 MPa, 33°), Dacitic lapilli tuff (6 MPa, 20 MPa, 27°), and Andesitic lapilli tuff (5 MPa, 5 MPa, 40°).

To verify the formation of induced fracture network, X-ray computed tomography (XCT) scans were performed on cylindrical samples before and after the fracturing experiments. The scans were conducted at approximately 23°C under atmospheric pressure, using a tube voltage of 120 kV and a tube current of 150 μA. Before the experiments, Honkomatsu and Emochi andesite samples were scanned with a voxel size of 25 μm, while the lapilli tuff samples were scanned with a voxel size of 12 μm. After the experiments, voxel sizes varied depending on the condition of the samples, with some requiring lower resolution (larger voxel sizes) due to significant deformations. To assist in identifying fractures in the lapilli tuff samples, deep learning segmentation was applied to post-experiment XCT sections using Dragonfly 3D visualization and analysis software (Object Research System Inc.). Additionally, to better understand the fracture characteristics in relation to the tuff component and lapilli, the interior of the fractured andesitic lapilli tuff sample was visually inspected under visible and ultraviolet (UV) light after had been impregnated with fluorescent resin.

The experiments were conducted using a conventional triaxial stress ($\sigma_1 > \sigma_2 = \sigma_3$; σ_1, σ_2, and σ_3 are the maximum, intermediate, and minimum principal stresses, respectively) experimental system combined with an acoustic emission (AE) measurement setup (Figure 1), described elaborately in Watanabe et al. (2017a, 2017b) and Takuma et al. (2024). The setup primarily includes a triaxial cell that used molten plastic as the confining pressure fluid, such as polyethylene (PE) melt for experiments conducted at 120–300°C. The triaxial cell also equipped with cylindrical axial stress pistons with central flow path and tubing for fluid injection. The fracturing fluid is injected using syringe pumps. In this system, the injected fluid is heated to the experimental temperature before reaching the sample, as confirmed by a thermocouple placed inside the injection tubing (Figure 1). The AE measurements system is Physical Acoustics Corporation two-channel data acquisition and digital signal processing PCI-2 system, equipped with an R15α sensor with a resonant frequency of 150 kHz. AE energy was computed by integrating the amplitude (voltage) over time, after background noise was subtracted, and was reported in arbitrary units (a.u.).

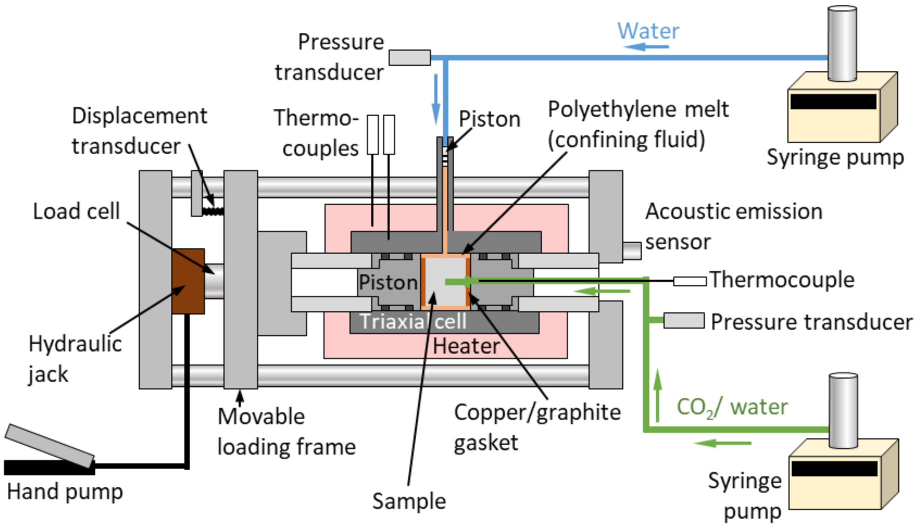

Figure 1. Design for the CO_2 and water-assisted CO_2 fracturing experiments under conventional-triaxial stress conditions.

To elucidate the influence of preexisting pore water on CO_2 fracturing, a CO_2 injection experiment (Experiment 1) was conducted on an initially water saturated Honkomatsu andesite sample (Table 1). The experiment was carried out at 250°C with 100 MPa axial stress, and 30 MPa confining pressure. In this experiment, CO_2 was initially present at 10 MPa inside the sample borehole for c.a. 20 min, during which the CO_2 could penetrate the rock matrix. The borehole was pressurized by injecting more CO_2 at 1 mL $\cdot$ min^{-1} from room temperature (c.a. 20°C). CO_2 penetration was expected to create complex fracture network at low fracture pressure (close to confining pressure value). The results of this experiment were then compared to those of CO_2 fracturing on dry Honkomatsu andesite fractured using the same injection strategy at identical condition, presented in Takuma et al. (2024).

Table 1. Sample materials, experimental conditions, and borehole pressurization methods.

Experiment	**Sample material**	**Temperature (°C)**	**Axial stress (MPa)**	**Confining pressure (MPa)**	**Borehole pressurization method**
1	Honkomatsu andesite	250	100	30	CO_2 injection
2	Honkomatsu andesite	250	100	30	Water compressed CO_2
3	Emochi andesite	250	80	30	Water compressed CO_2
4	Dacitic lapilli tuff	250	80	30	Water compressed CO_2
5	Andesitic lapilli tuff	250	80	30	Water compressed CO_2

In order to determine the effectiveness of water-assisted CO_2 fracturing, considering the influence of preexisting pore water, Experiment 2 was conducted on water-saturated Honkomatsu andesite at 250°C with 100 MPa axial stress, and 30 MPa confining pressure. In this experiment, CO_2 existed at 10 MPa within the sample borehole for 20 min. Then, the CO_2 pressure was increased by injecting water at 1 mL · min^{-1} (i.e., water-assisted CO_2 fracturing). In the present set up, water would arrive in the borehole about 240 s after the injection started. The CO_2 penetration was expected to create complex fracture network at low fracture pressure; these fractures were expected to be widened and propagated by the injected water. The outcomes of this experiment were then compared to those of experiment on dry Honkomatsu andesite fractured using the same injection strategy and condition presented in Takuma et al. (2024).

In order to determine the influence of rock texture on the fracturing characteristics, water-assisted CO_2 fracturing experiments were later conducted on water saturated Emochi andesite (Experiment 3), dacitic lapilli tuff (Experiment 4), and andesitic lapilli tuff (Experiment 5). These experiments were conducted at 250°C and 30 MPa confining pressure. Nevertheless, an axial stress of 80 MPa was used, to prevent rock failure prior to injections, considering the lower tensile strength, cohesion, and internal friction angles of the pyroclastic rocks. Based on Hubbert and Willis (1957), axial stress does not significantly affect fracture initiation. Experiment 3, 4, and 5 also employed the same injection strategy to that in Experiment 2.

3 Results and discussion

Time evolution of borehole pressure, AE energy, and cumulative AE energy, as well as post experiment XCT sections from Experiment 1 are presented in Figure 2. Fracturing probably initiated at 37 MPa borehole pressure, as indicated by slight increase in AE activity. After fracturing initiated, AE energy level was about 10 a.u. These responses were different from those in CO_2 fracturing of dry Honkomatsu andesite (Takuma et al. 2024), where fracturing initiation was indicated by more clear increase in AE activity, and the AE energy levels after fracturing were higher at about 30 a.u. The lower AE energy in Experiment 1 likely indicated an inhibited fracture propagation after their initiation, which later confirmed by the XCT sections that show a number of short, narrow fractures. To compare, fracture network formed in CO_2 fracturing of dry Hontkomatsu andesite consist of fewer, but longer and wider fractures (Takuma et al. 2024). The present experiment suggested that preexisting pore water inhibited fracture propagation in CO_2 fracturing.

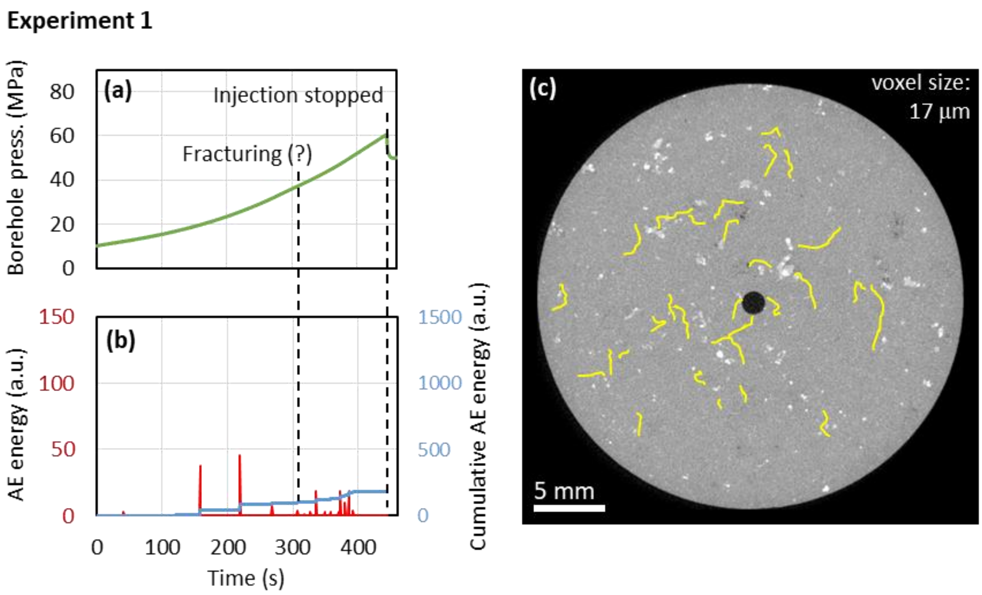

Figure 2. Results of Experiment 1: (a) borehole pressure, (b) AE energy (red) and cumulative AE energy (blue), (c) Post experimentation X-ray CT sections of the samples. Thin fractures are highlighted in yellow.

Takuma et al. (2024) implied that fracture widening and propagation require deformation of the surrounding unfractured rock matrix, which would include pore deformation (shrinkage). Based on Biot (1941) and Pimienta et al. (2017), it was hypothesized that if preexisting pore water, which is difficult to displace due to its higher viscosity, as well as less compressible than CO_2, became pressurized by the penetrating CO_2, the pores and the rock matrix would become less deformable. Therefore, while fractures may initiate in several areas, their propagation is impeded in water-saturated samples. In contrast, fractures in dry samples could extend further, with a few of them becoming wider and longer. This widening compressed the rock matrix, inhibiting the widening and propagation of the other fractures. However, these ideas could not be directly proven; computer simulations of the fracturing process might offer further clarification.

Time evolution of borehole pressure, AE energy, and cumulative AE energy from Experiment 2 are presented in Figure 3a. Fracturing probably initiated at 30 MPa borehole pressure, as indicated by increase in AE activity. After the fracturing initiated, AE activity and energy level in Experiment 2 were lower (value c.a. 15 a.u.) compared to those (c.a. 45 a.u.) of water-assisted CO_2 fracturing of dry Honkomatsu andesite sample under identical condition and injection method (Takuma et al. 2024); this indicated inhibition of fracture widening and propagation by preexisting pore water in Experiment 2. Nonetheless, the injected water appeared to be capable of widening and propagating the induced fractures, as fracture network formed in Experiment 2 (Figure 4a) was similar to that formed in water-assisted CO_2 fracturing of dry Honkomatsu andesite sample (Takuma et al. 2024). The fracture network consisted of few wider, longer fractures that connected the borehole and sample surfaces, as well as numerous narrower, shorter fractures. Slight difference was observed, where the longer fractures in Experiment 2 had fewer branches compared to those in dry Honkomatsu andesite sample from Takuma et al. (2024); this could be the remnant of fracturing inhibitory effect by preexisting pore water. Therefore, Experiment 2 showed that water-assisted CO_2 fracturing diminishes the inhibitory effect by preexisting pore water; this method is effective at inducing network of wide fractures in volcanic rock.

The time evolution of borehole pressure, AE energy, and cumulative AE energy from Experiments 3, 4, and 5 are presented in Figure 3b, 3c, and 3d, respectively. In these experiments, AE activity was detected from the start of injection, likely because the rock's high permeability allowed fluid to easily infiltrate, leading to significant deformation of the rock as a result of increased pore pressure (Takuma et al. 2024). Thus, the fracturing initiation were not clear. However, the fracturing initiation pressures were inferred based on slight increase in AE activity: Experiment 3, 31 MPa; Experiment 4, 33 MPa; and Experiment 5, 43 MPa. Increase in AE energy of several order of magnitude occurred in these experiments after water arrival, which indicate compressive deformation of the samples.

Post-experimentation XCT sections of the samples from Experiments 3, 4, and 5 revealed complex network of fractures comprised of wider, longer fractures, as well as thinner, shorter fractures (Figure 4b, 4c, and 4d). There was a tendency of fracture aperture increase with distance from borehole; this was due to larger circumferential compressive stress around the borehole compared to that near the sample surface. Nonetheless, the fractures were significantly wider than those formed in Experiment 2. Based on Sammis and Ashby (1986; Ashby and Sammis, 1990; Heap and Violay, 2021), it was speculated that the higher number of pores in pyroclastic rock samples allowed formation of fractures at many locations, which later coalesced into larger fractures. The injected water then widened and propagated these wider fractures.

There was also a tendency of increase in fracture aperture, noticeably in the longer factures, for Experiments 3, 4, and 5, which suggest that fracture aperture increase with clast size. In Experiments 4 and 5, wider fractures were observed within the tuff matrix, inside the lapilli, and most prominently at the boundary between the lapilli and the tuff component/matrix. This was later verified by visual inspection under visible and UV light of the resin-impregnated samples (Figure 5a, b), at planes similar or near those captured in the XCT scans (Figure 4c, 4d), with the wider fractures commonly found at the lapilli boundaries. We hypothesize that narrow fractures initially formed due to CO_2 infiltration along the boundaries of clasts of various sizes, as well as along pre-existing fractures or weak planes within the clasts. These boundaries likely represented weak planes containing interstitial pores. Due to the difference in deformability between the lapilli and the tuff matrix, the fractures at the lapilli boundaries may have undergone greater deformation, merged, and developed wider apertures compared to those within the tuff matrix. The subsequent infiltration and widening by the injected water would have been more effective in these larger fractures than the narrower ones within the tuff matrix, due to water higher viscosity than that of CO_2. Consequently, these wider fractures continued to widen and propagate. Again, this hypothesis could not be directly proven; therefore, computer simulations of the fracturing process might offer further clarification

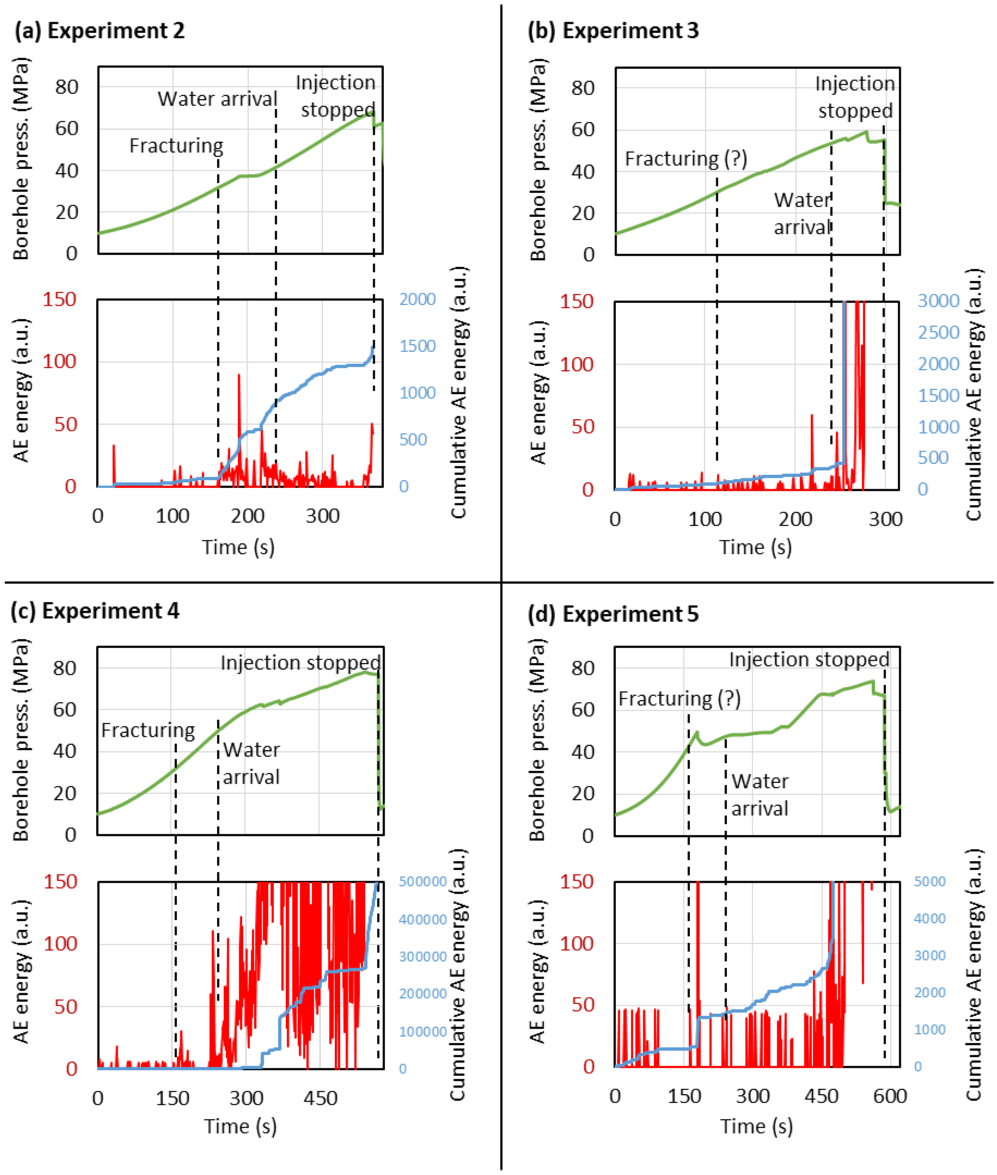

Figure 3. Time-evolution of borehole pressure, AE energy (red), and cumulative AE energy (blue) during injection in Experiment 2 (a), Experiment 3 (b), Experiment 4 (c), and Experiment 5 (d).

The current experiments demonstrate that fracture aperture tends to increase with porosity and grain or clast size during water-assisted CO_2 fracturing in volcanic rock. This suggests that pyroclastic rocks containing larger clasts, such as agglomerates, lapillistones, and lapilli tuffs, may experience greater permeability enhancement. These rocks could be ideal for geothermal reservoirs, particularly in CO_2-based enhanced geothermal systems, where maintaining an optimal mass flow rate is crucial for balancing energy production and reservoir longevity (Biagi et al., 2015). The differences in fracturing characteristics with rock texture suggest that water-assisted CO_2 fracturing could lead to variations in hydraulic properties, such as heterogeneity in overall permeability, across different volcanic rock types in a geothermal environment. Therefore, evaluating the geometry and distribution of volcanic rocks (e.g., distribution of lava, distribution of pyroclastic density current deposit) prior to fracturing is crucial. Gaining this understanding would aid in predicting the hydraulic properties within the stimulated area and in identifying the most effective locations for placing injection and production wells to maximize energy output.

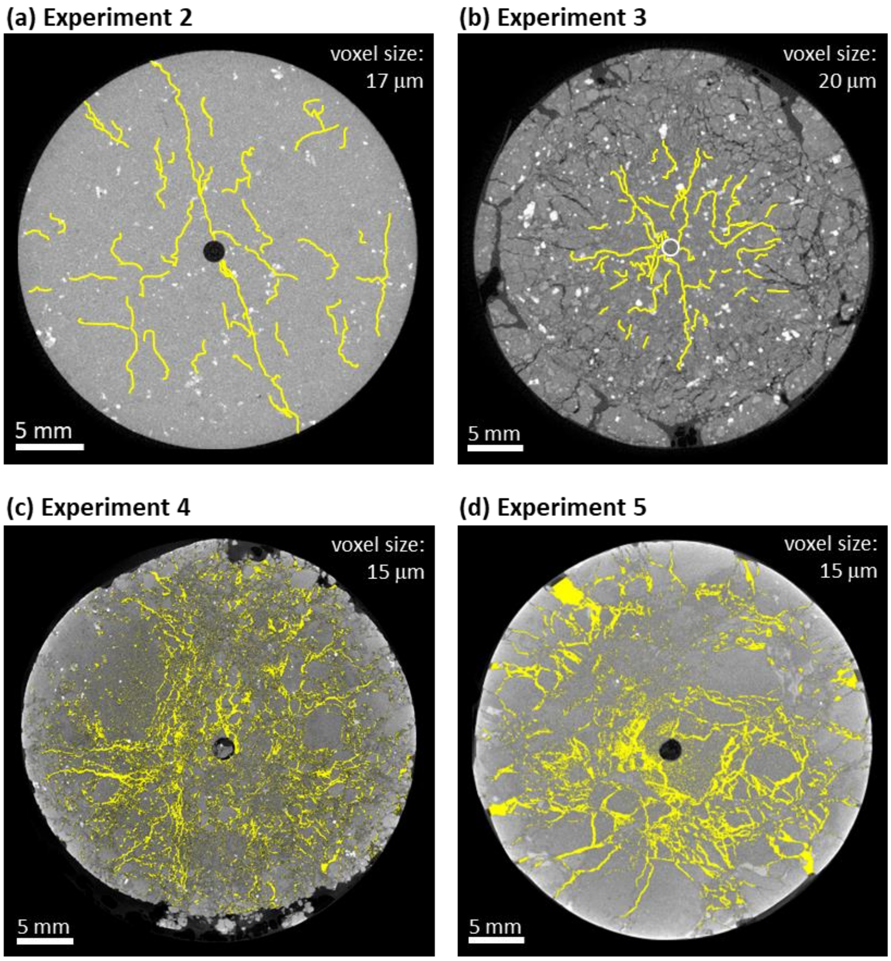

Figure 4. Post experimentation X-ray CT sections of the samples from Experiment 2 (a), Experiment 3 (b), Experiment 4 (c), and Experiment 5 (d). Narrow fractures are highlighted in yellow in Experiment 3. Yellow lines in Experiment 4 and 5 indicate fractures identified by deep-learning segmentation.

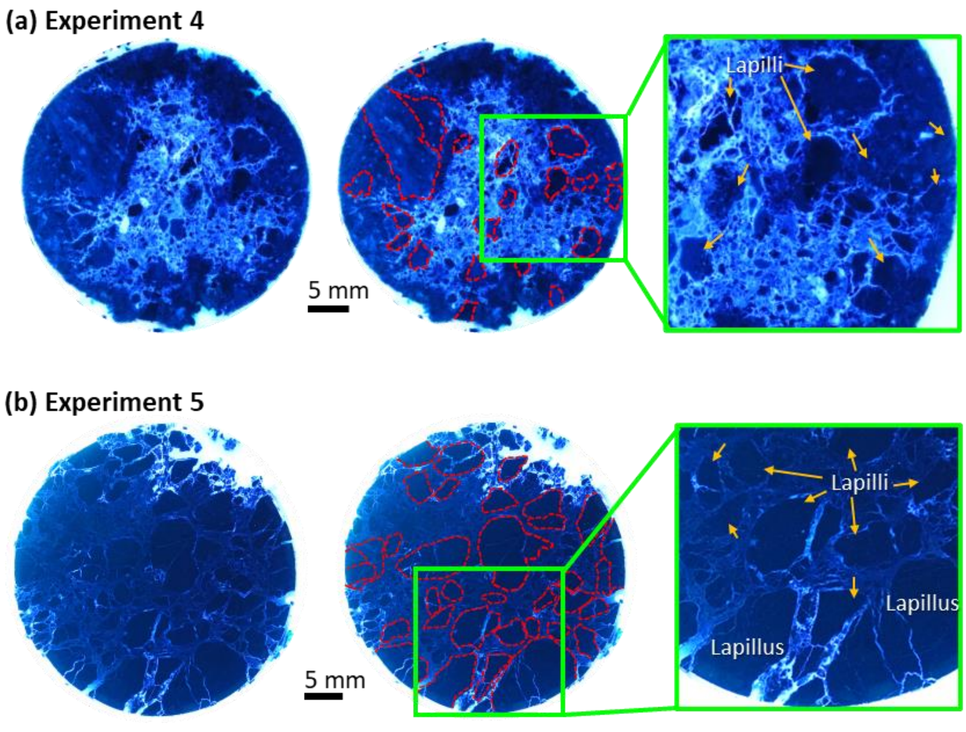

Figure 5. UV light photographs of fluorescence resin-impregnated samples from Experiments 4 (a) and 5 (b), exposed at planes close to those shown in Figure 4 (b, c). Dashed red lines enclose lapilli recognizable under visible light.

4 Conclusions

Through a set of experiments, this study revealed that water-assisted CO_2 fracturing effectively achieves complex network of wide fractures in various volcanic rocks under geothermal conditions. At first, it was demonstrated that preexisting pore water inhibits the widening and propagation of fractures induced by CO_2. Nevertheless, the injected water in water-assisted CO_2 fracturing widened and propagated the CO_2 injection-induced fractures, diminishing the inhibitory effect by preexisting pore water. It was also demonstrated that porosity and rock texture influence the characteristics of fracture network induced by water-assisted CO_2 fracturing. Porous volcanic rock, such as tuff, retained wider fractures compared to tight volcanic rock, such as lava. In pyroclastic rocks, it was shown that fracture aperture and length increased with clast size, where the wider fractures tended to be located at the boundaries of large clasts. This suggests that pyroclastic rocks containing large clasts (agglomerates, lapillistones, lapilli tuffs) are preferable for hosting geothermal reservoirs.

Acknowledgement

This study was commissioned by JOGMEC and supported by the JST FOREST Program (no. JPMJFR216Y, Japan). This study was partially supported by the Japan Society for the Promotion of Science through Grants-in-Aid for Scientific Research (S) (No. 22H04932), Scientific Research (A) (No. 21H04664), Scientific Research (B) (Nos. 22H02015, 23K23283, 23H01903, and 24K01412), Challenging Research (Pioneering; No. 21K18200), and Early-Career Scientists (No. 24K17139). The experimental system was manufactured by the Toei Scientific Industrial Co., Ltd, Natori City, Japan.

References

Ashby, M.F., Sammis, C.G., 1990. The damage mechanics of brittle solids in compression. *Pure Appl. Geophys. 133*, 489–521.

Biagi, J., Agarwal, R., Zhang, Z., 2015. Simulation and optimization of enhanced geothermal systems using CO_2 as a working fluid. *Energy. 86*, 627–637.

Biot, M.A., 1941. General theory of three‐dimensional consolidation. *J. Appl. Phys*. 12, 155‐164.

Eggertsson, G.H., Lavallée, Y., Kendrick, J.E., Markússon, S.H., 2020. Improving fluid flow in geothermal reservoirs by thermal and mechanical stimulation: The case of Krafla volcano, Iceland. J. Volcanol. Geotherm. Res. 391, 106351.

Heap, M.J., Violay, M.E., 2021. The mechanical behaviour and failure modes of volcanic rocks: a review. *Bull. Volcanol. 83*, 33.

Hubbert, M.K., Willis, D.G., 1957. Mechanics of hydraulic fracturing. *Trans. AIME. 210*, 153–168. 10

Pimienta, L., Fortin, J., Guéguen, Y., 2017. New method for measuring compressibility and poroelasticity coefficients in porous and permeable rocks. *J. Geophys. Res.: Solid Earth. 122*, 2670–2689.

Pramudyo, E., Takuma, K., Watanabe, Y., Sakaguchi, K., Maeda, Y., Ogata, S., Sueyoshi, K., Wang, J., Osato, K., Terai, A., & Watanabe, N. (2024). Characteristics and effectiveness of water-assisted CO_2 fracturing for creating geothermal reservoirs in volcanic rocks. *Geoenergy Science and Engineering, 243*, 213280.

Sammis, C.G., Ashby, M.F., 1986. The failure of brittle porous solids under compressive stress states. *Acta Metall. 34*, 511–526.

Takuma, K., Maeda, Y., Watanabe, Y., Ogata, S., Sakaguchi, K., Pramudyo, E., Fukuda, D., Wang, J., Osato, K., Terai, A., Watanabe, N., 2024. CO2 fracturing of volcanic rocks under geothermal conditions: Characteristics and process. *Geothermics. 120*, 103007.

Watanabe, N., Numakura, T., Sakaguchi, K., Saishu, H., Okamoto, A., Ingebritsen, S.E., Tsuchiya, N., 2017a. Potentially exploitable supercritical geothermal resources in the ductile crust. *Nat. Geosci. 10*, 140–144.

Watanabe, N., Egawa, M., Sakaguchi, K., Ishibashi, T., Tsuchiya, N., 2017b. Hydraulic fracturing and permeability enhancement in granite from subcritical/brittle to supercritical/ductile conditions. *Geophys. Res. Lett. 44*, 5468–5475.

Yoshioka, K., Pasikki, R., & Stimac, J. (2019). A long term hydraulic stimulation study conducted at the Salak geothermal field. *Geothermics, 82*, 168-181.